Toward Understanding the Influence of Intermolecular Interactions and Molecular Orientation on the Chemical Enhancement of SERS

ARTICLE *in* THE JOURNAL OF PHYSICAL CHEMISTRY A · AUGUST 2013

Impact Factor: 2.69 · DOI: 10.1021/jp403458k · Source: PubMed

3 AUTHORS, INCLUDING:

Steve D. Christesen
United States Army
80 PUBLICATIONS **540** CITATIONS

THE JOURNAL OF PHYSICAL CHEMISTRY A

Article

pubs.acs.org/JPCA

Toward Understanding the Influence of Intermolecular Interactions and Molecular Orientation on the Chemical Enhancement of SERS

Jerry Cabalo*

CB Systems Integration, Edgewood Chemical Biological Center (ECBC), 5183 Blackhawk Road, RDCB-DRI-I, Aberdeen Proving Ground, Maryland 21010, United States

Jason A. Guicheteau and Steven Christesen

Laser Standoff Branch, Edgewood Chemical Biological Center (ECBC), 5183 Blackhawk Road, RDCB-DRD-L, Aberdeen Proving Ground, Maryland 21010, United States

ABSTRACT: Implementation of SERS as an analytical technique is limited because the factors that govern the enhancement of individual vibrational modes are not well understood. Although the chemical effect only accounts for up to two orders of magnitude enhancement, it can still have a significant impact on the consistency of chemical spectral signatures. We report on a combined theoretical and experimental study on the benzenethiol on silver and 4-mercaptophenol on silver systems. The primary and unique finding was that for the benzenethiol on silver system the inclusion of interaction between multiple benzenethiol analyte molecules was essential to account for the relative enhancements observed experimentally. An examination of the molecular orbitals showed sharing of electron density across the entire model of multiple benzenethiol molecules mediated by the metal atoms. The addition of multiple 4-mercaptophenol molecules to the theoretical model had little effect on the predicted spectra, and we attribute this to the fact that a much larger model is necessary to replicate the networks of hydrogen bonds. Molecular orientation was also found to affect the predicted spectra, and it was found that an upright position improved agreement between theoretical and experimental spectra. An analysis of the vibrational frequency shifts between the normal Raman spectrum of the neat compound and the SERS spectrum also suggests that both benzenethiol and 4-mercaptophenol are in an upright position.

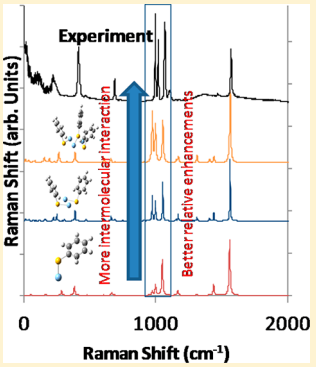

INTRODUCTION

Surface-enhanced Raman scattering (SERS) is an analytical technique with much promise. Whereas standard Raman spectroscopy is a powerful technique because of its specificity, it is limited with respect to sensitivity. Enhancement factors up to six orders of magnitude are commonly observed in SERS.[1] Despite the high degree of enhancement, SERS spectra can be difficult correlate with normal Raman spectra. The fact that multiple processes contribute to the enhancement complicates the interpretation of the SERS spectra and limits the full exploitation of the SERS technique.

SERS is believed to have two major processes that contribute to the enhancement, one from the local electric field effects (EM) arising from surface plasmon resonance in the metal substrate and the other arising from a chemical effect that contributes up to two orders of magnitude of enhancement.[2] While the plasmonic, electric field effect accounts for most of the enhancement and can be understood in terms of a simple surface selection rule, the chemical effect can greatly affect the relative enhancements of the different frequencies in the spectrum. As a result, the peaks in a SERS spectrum can be difficult to relate to the unperturbed Raman spectrum of the neat compound. The chemical effect can be viewed as arising from modification of the electronic molecular structure of the analyte by the SERS substrate.[3−7] The result is a complex between the metal and the analyte molecule that has electronic, or charge transfer, states that are much lower in energy than analyte molecule alone.[8,9] The analyte molecule plus metal atom complex structure must be considered as a whole to understand the SERS spectra.[5,8,10−12] Using the sum of states formulation[13,14] of the dynamic polarizability as a framework, these charge-transfer states can be viewed as contributing to the sum of states for the Raman signal, and when the excitation laser is in resonance with the charge-transfer states, even greater enhancement is possible from one of these states.[1,6] The chemical enhancement for each normal mode is sensitive to changes in the electronic structure of the analyte molecule-metal complex, which is in turn sensitive to orientation to the surface,[15] surface defects,[16] or even the presence of other adsorbates.[17] The changes in the contribution to the chemical enhancement that arise when the local molecular orientation and environment modify the electronic structure of the metal−analyte molecule complex are a primary interest of the present study.

Received: April 8, 2013
Revised: August 1, 2013

   dx.doi.org/10.1021/jp403458k | J. Phys. Chem. A XXXX, XXX, XXX−XXX

The relationship between molecular orientation on a surface and chemical enhancement is still unclear. Several combined theoretical and experimental studies have been reported that show that the local environment around an analyte molecule on the SERS substrate is important to understanding the Raman enhancement each vibrational mode experiences. In an electron energy loss (EEL) and Raman study of pyromellitic dianhydride (PMDA) on the 100 and 111 crystal faces of Cu,[18] PMDA on the different crystal faces exhibited different SERS responses. The EEL spectra revealed that the electronic excited-state structure changed depending on which crystal face was observed. This study demonstrated the sensitivity of the SERS response to the modifications to electronic states arising from chemisorption. However, this study did not investigate the influence of molecular orientation further on the chemical enhancement. Another study[15] compared experimental SERS data to models of analyte molecule−metal complexes and demonstrated that small models of the analyte molecule−metal complex of <10 metal atoms were sufficient to simulate SERS spectra in good agreement with experiment. That result demonstrated that small models of the analyte-metal complex can depict the metal-induced modifications to the excited electronic state structure. However, a clear relationship between orientation and chemical enhancement did not emerge. A theoretical study of pyridine and substituted pyridines on silver clusters[8] studied the relationship between molecular properties and the SERS response while maintaining a constant molecular orientation, but again, orientation was not a focus of this study. The Raman spectra and charge transfer were calculated for 22 different combinations of functional groups and locations on the pyridine ring. It was revealed that the degree of chemical enhancement depends on the difference in energy between the highest occupied molecular orbital (HOMO) of the metal cluster and the lowest unoccupied molecular orbital (LUMO) of the molecule instead of the magnitude of transferred charge. The theoretical results of the above studies where the electromagnetic portion of the enhancement is neglected generally explain the observed SERS spectra, but some ambiguity remains because of the difficulty of treating both of the effects within the same model. One study that included both the EM and chemical enhancements was reported using a mixed quantum-classical model to simulate the EM enhancement from a metal nanoparticle.[19] They reported preferential adsorption to the apexes and edges over the faces of their icosahedral metal nanoparticle model. However, orientation of the analyte molecule was again not a focus of that study. In another effort to study the chemical effect of SERS as well as the effect of molecular orientation, graphene-enhanced Raman scattering (GERS) has been used to measure chemical effects without the presence of EM effects. However, the results of the GERS study might not be generally applicable. Chemical interactions as strong as thiols or amines on gold are not possible with GERS. Only interactions between the aromatic graphene and isoindole groups on the copper phthalocyanine were investigated.[20] Because of the remaining ambiguity, it is the objective of this study to investigate the relationship between molecular orientation and vibrational mode enhancement in SERS. At the same time, we wish to examine the effect of molecular polarity.

To accomplish this objective, we examined the well-known[21−24] benzenethiol and 4-mercaptophenol on silver systems, where the hydroxyl group at the para position relative to the thiol group on the benzyl ring increases polarity. Extensive work has been done to characterize the structure of these chemicals that form a self-assembled monolayer (SAM) on silver, and the surface structure is understood.[21] Our initial hypothesis was that the change in polarity in the molecule would greatly influence the enhancement in the SERS spectrum by changing the magnitude of charge transfer. We expected that interaction between the metal substrate and the analyte molecule alone would completely explain the chemical enhancement and that proper representation of that interaction would result in agreement between theory and experiment. Within each of the models, we had expected the size of the metal cluster to be the primary driver for correctly depicting the environment around the analyte molecule. However, results from this study reinforce the idea that the structure of the entire analyte molecule−metal complex has to be considered. For modeling some systems, multiple analyte molecules must be considered in the molecular−metal complex to correctly interpret the SERS spectrum. Although many of the models used in this study are similar to those already reported, a key difference is the focus on interaction between analyte molecules on the surface.

EXPERIMENT

Silver nanoparticle suspensions were prepared following a modified procedure of Lee and Meisel[25] as previously described.[26] In a 1 L three-necked round-bottomed flask, 90 mg of silver nitrate (99+ %, SigmaAldrich) were dissolved in 400 mL of deionized water (18.3 MΩ). The solution was brought to a boil with constant stirring, and an additional funnel was used to deliver 10 mL of 1% aqueous sodium citrate upon boiling. Heating and stirring were maintained for 45 min after the addition of citrate, at which time the reaction flask was removed from heat and allowed to cool to room temperature. The resulting nanoparticle suspensions appeared yellowish brown with an electronic absorption λ_{max} of 400 nm and an average full width at half-maximum of 65 nm with an average particle size of 36 nm. Bezenethiol and 4-mercaptophenol were purchased from SigmaAldrich and used without modification. SERS measurements were made on an EIC Echelle spectrograph fiber-optically coupled using an InPhotonics RamanProbe operating at 785 nm with 1 cm^{-1} resolution at 150 mW. For both benzenthiol and 4-mercaptophenol, final concentrations of 100 μM were examined in 400 μL of colloid with 10 s acquisition times.

Quantum-mechanical calculations were performed using Gaussian 2009 revision C.01[27] on neat benzenethiol and 4-mercaptophenol and on these molecules chemically bound to Ag clusters with one, three, five, and seven atoms. The hydrogen attached to the thiol group in the free molecule was not included in the calculation and was considered to be already detached. Two geometries were explored for the three-Ag-atom cluster calculations. Where the three Ag cluster formed an equilateral triangle, one geometry attached the sulfur of the benzenethiol and 4-mercaptophenol to the apex of the cluster (denoted as (A) in Figures 2 and 4), and the other geometry attached it to a side of the triangle. For the five- and seven-atom metal clusters, the atoms were laid out in a plane to approximate a surface, although these sheetlike clusters were allowed to relax without constraints during geometry optimization. All calculations involving the silver metal clusters were performed with the hybrid B3LYP functional with the LANL2DZ double-ζ basis set with relativity-corrected effective core potentials. To explore basis set effects, we performed

dx.doi.org/10.1021/jp403458k | J. Phys. Chem. A XXXX, XXX, XXX−XXX

additional calculations on molecular benzenethiol and 4-mercaptophenol and the B3LYP functional with the triple ζ 6-311+G(d,p) and correlation-corrected aug-cc-pVTZ basis sets. Only metal cluster sizes that had closed-shell electronic structures were examined so that open-shell unrestricted results were not considered for the study on metal cluster size. Excitation frequency-dependent spectra were calculated using the coupled perturbed Hartree−Fock equations at 785 nm for all calculated Raman spectra. The vibrational wavenumbers have been scaled by a factor of 0.961 for the B3LYP/LANL2DZ method.[28] Time-dependent DFT (TD-DFT) calculations for the lowest 200 electronic states were performed to investigate the influence of the metal−molecule interaction on the electronic structure for the benzenethiol and 4-mercaptophenol. The TD-DFT calculations were also used to confirm that the frequency-dependent Raman spectra were calculated in a nonresonant condition only because the Gaussian 2009 code cannot calculate resonant Raman spectra. Only the singlet transitions were calculated. To examine different molecular orientations, the Raman spectrum was calculated from a model containing two benzenethiol molecules and a seven-Ag-atom cluster and from a model containing two 4-mercaptophenol molecules with a seven-Ag-atom cluster, where the open-shell unrestricted calculation was performed. The presence of a second molecule during geometry optimization forced one molecule into an upright position and brought the ring of the other molecule into contact with the metal cluster. Raman signal was attributed to a particular molecule in the model by weighting the Raman scattering factor by the square of the Cartesian atomic displacements of the atoms in that molecule. In general, the normal modes separated cleanly between the two analyte molecules.

The interaction between analyte molecules mediated by the metal surface was modeled with one to three analyte molecules (both benzenethiol and 4-mercaptophenol), where each molecule was associated with a single silver metal atom. The clusters of three analyte molecules and three metal atoms and two analyte molecules with two metal atoms were permitted to relax without constraints during the geometry optimization. A number of other calculations were also attempted with hybrid quantum mechanical/classical mechanical (QM:MM) methods and with larger systems with geometry constraints to capture molecular behavior on a realistic surface, yet these calculations did not converge to an optimized structure.

DISCUSSION

In the case where nonresonant spectra were measured with 785 nm excitation, there was agreement between experimental measurements and theoretically predicted spectra from simple single -molecule models using the B3LYP/LANL2DZ method, as shown in Figure 1. Overall, agreement between theory and experimental measurement is good. The in-plane ring deformations of 4-mercaptophenol at 623, 787, 1057, 1221, 1563, and 1585 cm^{-1} compare well with the experimental absorptions at 634, 813, 1076, 1249, 1589, and 1602 cm^{-1}, respectively. Modest disagreement between theory and experiment arises from modes involving hydrogen bends. The modes at 797 and 823 cm^{-1} are nearly identical and involve in-plane hydrogen bends on different sides of the molecular model, where a single feature appears in the measurement at 828 cm^{-1}. The theoretical peak at 877 cm^{-1} involving bending of the thiol hydrogen differs from the experimental peak at 918 cm^{-1} by 41 cm^{-1} and overestimates the intensity. The peaks at 1120 and

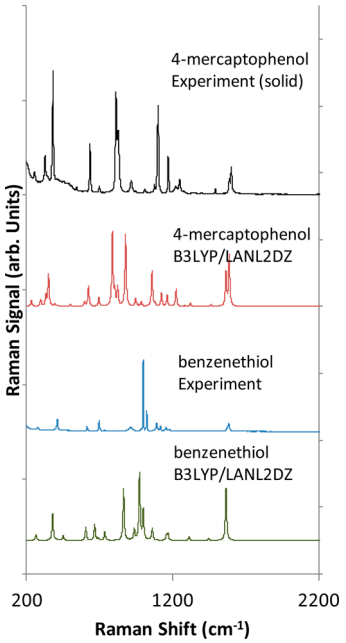

Figure 1. Benzenethiol and 4-mercaptophenol measurement (neat) versus theory.

1158 cm^{-1} arise from in-plane hydrogen bending on the ring and hydroxyl group, and only a single peak at 1170 cm^{-1} appears in the same region of the experimental spectrum. Either these two modes are close in frequency and appear as a single peak in the experimental measurement or the frequency of the hydroxyl hydrogen bend is greatly underestimated. The same pattern is followed for benzenethiol. Ring deformations predicted at 604, 665, 973, 996, 1057, and 1563 cm^{-1} lie within 35 cm^{-1} of the experimental values at 617, 698, 924, 1000, 1092, and 1584 cm^{-1}, respectively. Modest disagreement modeled at 733, 863, and 935 cm^{-1}arises from out-of-plane hydrogen bends. Significant disagreement between the model and experiment was in the S−H stretching frequency at 2566 cm^{-1} (not shown in Figure 1), where theory differed from experiment by 180 cm^{-1} for benzenethiol and 200 cm^{-1} for 4-mercaptophenol. Calculations on neat benzenethiol and 4-mercaptophenol using the B3LYP/6-311+G(d,p) and the B3LYP/aug-cc-pVTZ methods exhibited closer agreement for this mode; however, the LANL2DZ basis set was used for all calculations because it was adequate for the other modes and was suitable for calculations containing Ag atoms.

Figures 2 and 3 show predicted SERS spectra compared with experiment for benzenethiol and 4-mercaptophenol, respectively. For all spectra displayed, they are all scaled to facilitate the comparison of the relative enhancement in the spectra. The addition of metal atoms generally increased the total overall enhancement in that one Ag atom greatly enhanced the spectrum and three Ag atoms enhanced the spectrum even more, but there was no monotonic increase in calculated Raman activity as the metal cluster size was increased nor was there a clear dependence on the relative enhancements on the number of atoms in the metal cluster. For example, for benzenethiol on silver, both the model with a single metal atom and the model with seven metal atoms matched to the experiment more closely than the three- and five-metal-atom clusters. The three-metal-atom cluster with geometry A (with the sulfur attached to the apex of the cluster and the benzyl ring

dx.doi.org/10.1021/jp403458k | J. Phys. Chem. A XXXX, XXX, XXX−XXX

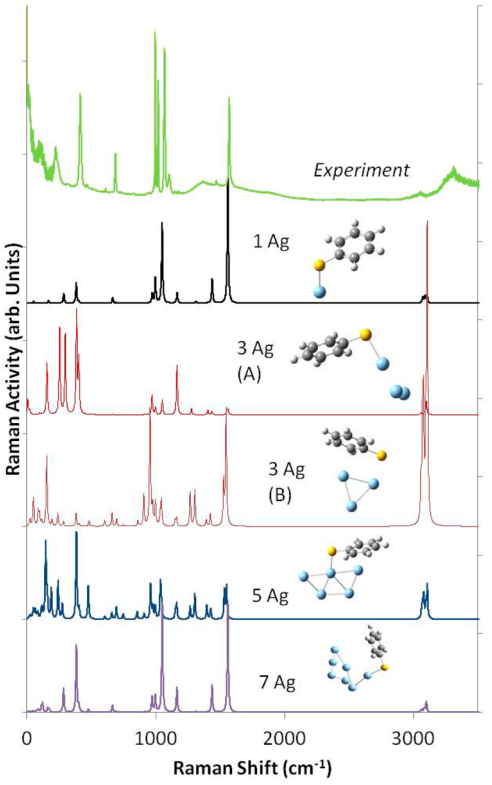

Figure 2. Comparison of experiment and a series of theoretical spectra generated from benzenethiol associated with small silver clusters with one, three, five, and seven atoms. Two orientations (A and B) have been calculated for the three-atom cluster.

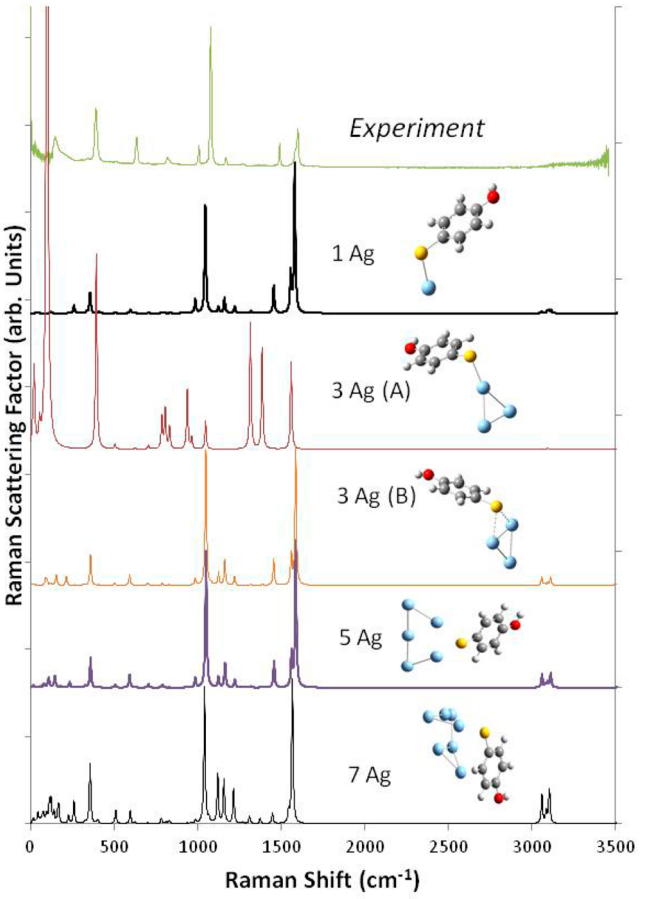

Figure 3. Comparison of experiment and a series of theoretical spectra generated from 4-mercaptophenol associated with small silver clusters with one, three, five, and seven atoms. Two orientations (A and B) have been calculated for the three-atom cluster.

far from the metal) and the five-metal-atom cluster bore little resemblance to the data. For the three-metal-cluster with geometry B, the spectrum resembled the experiment more closely than geometry A, yet the benzyl ring is quite close to one of the atoms in the cluster and peaks that are predicted from this model do not appear in the experimental spectrum. In other words, the enhancement each vibrational mode experiences depends greatly on the geometry between the metal cluster and the analyte molecule.

Similar observations can be made in the case of 4-mercaptophenol. The spectra predicted from the analyte associated with a single silver atom, and five silver atoms (these spectra are nearly identical) resembled the experimental spectrum the closest. As with benzenethiol, the spectrum predicted from the 4-mercapto phenol attached to the apex of the three-metal-atom cluster (labeled as 3 Ag (B) in Figure 4) had no resemblance to the experiment, showing enhanced peaks at greatly different frequencies. Interestingly, the geometry with the sulfur attached at the base of the triangular cluster gave results more consistent with the models with one, five, and seven silver atoms.

Many of these observations can be understood when the modifications to the electronic structure induced by the metal cluster are taken into account. Figures 4 and 5 show the results of TD-DFT calculations performed on the same molecular models of benzenethiol and 4-mercaptophenol used to calculate the spectra in Figures 2 and 3. To show that the optical absorptions by the charge-transfer states are no longer red-shifted as atoms are added to the metal cluster, we show additional results for 9, 11, and 13 Ag metal clusters for benzenethiol in Figure 4. The 200 lowest singlet electronic states were calculated for each model. Figures 4 and 5 show both stick spectra with optical wavelength versus oscillator strength and the theoretical UV–vis absorption spectrum generated by fitting each absorption with a 20 nm fwhm Gaussian line shape. The bottom traces show the calculated electronic structure of the free molecule, and progressive traces show the results of adding Ag atoms to the associated cluster. As metal atoms are added, the theoretical optical absorption spectrum is red-shifted. We attribute the lower energy states of the analyte molecule–silver cluster complex to the charge-transfer states.

For benzenethiol, by the time a silver cluster of nine atoms is reached, the optical absorption envelope is centered at ~325 nm and there is no additional red-shifting of the main absorption. The predicted optical absorption does not change much as the cluster size is increased to 13 atoms. The results show that additional metal atoms to the analyte molecule–metal cluster complex do not greatly modify the electronic structure and that clusters of this size are sufficient to simulate the chemical enhancement part of SERS.

Another important observation to be made from Figures 4 and 5 is that isolated charge-transfer states appear at wavelengths outside the main cluster of charge-transfer states and that the oscillator strengths of these states are much weaker than those within the main cluster of charge-transfer states. The variation of the location of the charge-transfer states as the

dx.doi.org/10.1021/jp403458k | J. Phys. Chem. A XXXX, XXX, XXX–XXX

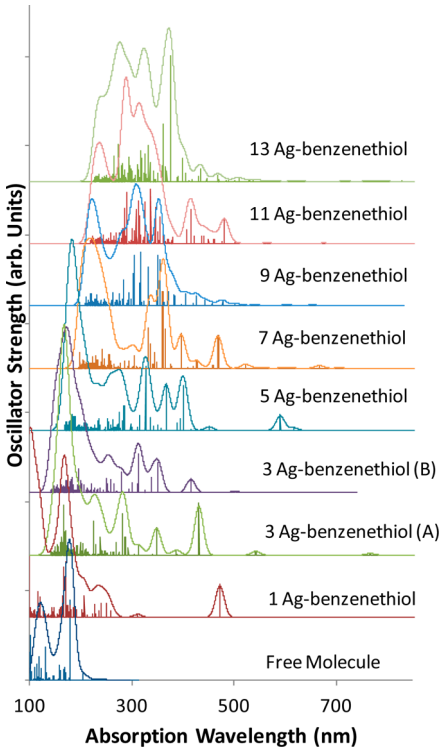

Figure 4. Optical absorptions for benzenethiol-silver clusters, for 1, 3, 5, 7, 9, 11, and 13 Ag atom clusters.

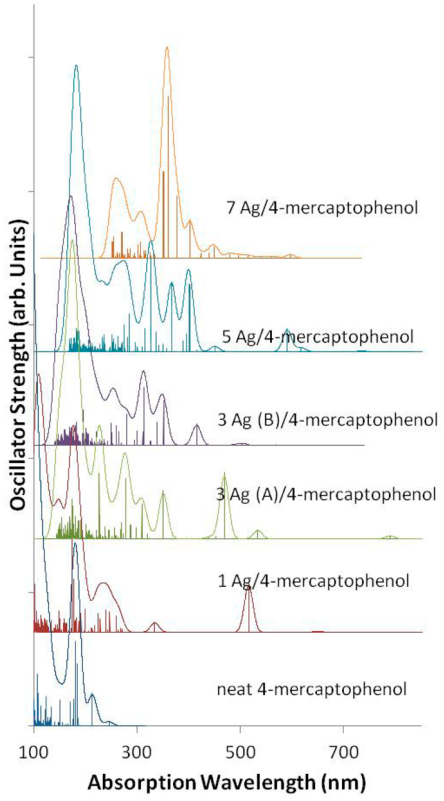

Figure 5. Optical absorptions for 4-mercaptophenol-silver clusters for one, three, five, and seven Ag atom clusters.

metal cluster is changed illustrates that these states are very sensitive to the geometry of the metal cluster−analyte molecule complex. The comparison of the two geometries of the three-Ag-atom cluster shows that the electronic structure, especially with respect to the isolated charge-transfer states, is sensitive to the orientation of the benzenethiol relative to the metal cluster. For the A geometry where the sulfur is attached to the apex of the cluster, there is an isolated electronic state at 760 nm for benzenethiol and 789 nm for 4-mercaptophenol. For the B geometries with the benzenethiol and 4-mercaptophenol attached at the base of the triangle formed by the metal atoms, the closest charge-transfer state is at 500 nm. As shown by the differences between the Raman spectra from the A and B geometries of both benzenethiol and 4-mercaptophenol, preresonance with the states at 760 and 789 nm, respectively, can drastically change the relative enhancement for each normal mode.

The effect of the isolated low-energy charge-transfer states is overemphasized in the model relative to the experiment because the experimental measurement is performed on a large ensemble of molecules and the models all involve a single molecule. The oscillator strengths and energies of the isolated charge-transfer states are highly sensitive to the geometry of the analyte molecule relative to the metal substrate, and these states do not contribute significant absorption to the overall optical spectrum. Although the five-Ag-atom cluster benzenethiol model has a similar geometry to the three-Ag B geometry, the isolated charge-transfer states for these models pictured are significantly different. We expect the average effect of these states over a large ensemble of molecules to be negligible. For the benzenethiol and 4-mercaptophenol molecular models associated with a single Ag atom, the two lowest electronic states at ∼650 and ∼475 nm (both molecules) are far from the 785 nm excitation frequency modeled. Preresonance with these low-lying charge-transfer states is avoided, and their contribution does not dominate the Raman spectrum. We can infer that the reason some models, such as the single- or seven-Ag-atom models of benzenethiol and 4-mercaptophenol, agree with experiment better than other models is that resonance and preresonance with isolated charge-transfer states is avoided. The isolated charge-transfer states also affect the predicted absolute enhancement. Rather than seeing a clear dependence of enhancement on the number of metal atoms in the cluster, the enhancement seems to depend more on the proximity of charge-transfer states to the excitation wavelength. For the experimental measurement, the excitation laser may be in resonance with the charge-transfer states of a few analyte molecules, but the effect of the weak oscillator strength of the isolated charge-transfer states may average out and not appear in the measured spectrum. Models of the molecular analyte and metal cluster complexes that avoid resonance and preresonance with these states have a better chance of agreeing with data than models that overemphasize single charge-transfer states close to the simulated excitation wavelength.

To investigate the effects of orientation, we attempted to model the SERS spectrum with the analyte molecule in arbitrary up or down positions relative to the metal cluster. It proved to be difficult to force single-analyte molecule models into arbitrary positions relative to the metal cluster. The models shown in Figures 6 and 7 include two analyte molecules attached to the seven-silver-atom cluster optimized in previous calculations to accomplish thi,. Following unconstrained geometry optimization for benzenethiol and 4-mercaptophenol models, one analyte molecule was forced into an upright position (labeled “up”), and the ring of the other molecule was brought into proximity with the metal cluster, (labeled

dx.doi.org/10.1021/jp403458k | J. Phys. Chem. A XXXX, XXX, XXX−XXX

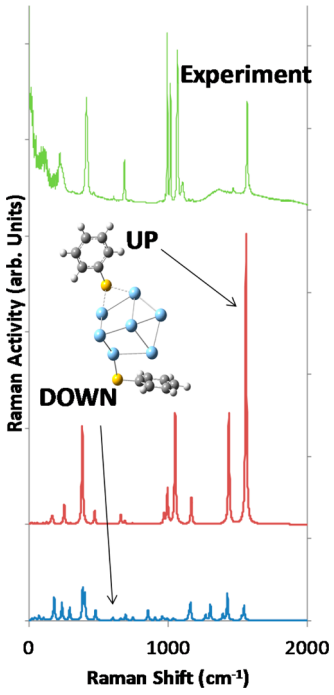

Figure 6. Comparison of experimental and theoretical SERS spectra for two orientations relative to the substrate surface from benzenethiol.

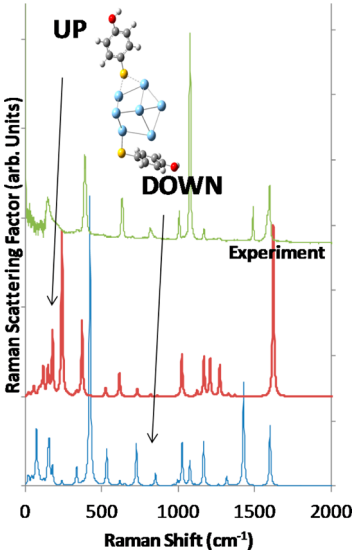

Figure 7. Comparison of experimental and theoretical SERS spectra for two orientations relative to the substrate surface from 4-mercaptophenol.

"down"). The Raman scattering factors from each of the molecules in the model were separated using the normal mode vectors reported by Gaussian. The sum of squares of the atomic motion vectors was normalized to one so the normal mode vectors could be used to weight the contribution to the overall Raman spectrum from each individual molecule. For the benzenethiol results in Figure 6, it can be seen that for the spectrum predicted from the down position many of the modes are relatively enhanced. In contrast, fewer modes are visible in the up spectrum, where most of these peaks correspond to peaks in the experimental spectrum. This result is consistent with published results[21] for silver, where the ring makes an angle of 24° relative to the vector normal to the surface. A similar structure is obtained for 4-mercaptophenol. Again, the down spectrum shows a greater number of frequencies experiencing relative enhancement than is shown in the experimental spectrum.

We attribute the differences between the down and up spectra of both benzenethiol and 4-mercaptophenol to the contact between the phenyl ring and the metal cluster. The molecular model of benzenethiol on a five-Ag-atom cluster shows the phenyl ring approaching one of the metal atoms. Not surprisingly, the resulting spectrum shows not only peaks present in the single-Ag-atom model at 1557, 1441, 1051, 994, 970, and 384 cm^{-1} but also many additional peaks (e.g., at 1393, 1306, and 1264 cm^{-1}). The same holds true for benzenethiol and the B geometry of the three-Ag-atom model, where near contact with the metal cluster causes many more Raman peaks to appear. This is consistent with the down spectra, which have many more peaks and a different relative enhancement pattern than the up position. The same observation can be made from the seven-Ag-atom cluster model associated with 4-mercaptophenol. Although the resulting spectrum from this model generally resembles the other models (except the A geometry of the three-Ag-atom cluster model), significant Raman peaks can be observed at 1118, 1152, and 1216 cm^{-1}. Perhaps contact between the phenyl ring and the metal cluster enhances out-of-plane motions in addition to in-plane ring deformations. On the basis of the previous TD-DFT calculations on single analyte molecules associated with metal clusters, we can attribute the changes in absolute enhancement between the up and down spectra to the orientation-dependent change in electronic structure.

A comparison of the normal-mode frequencies and intensities from the two analyte molecules within the same previously described theoretical model can also be used to examine the influence of molecular orientation on the vibrational frequencies. Tables 1 and 2 show a selection of the more intense vibrational frequencies, intensities, and descriptions of the normal mode motions of the up and down orientations as well as for the isolated molecule for benzenethiol and 4-mercaptophenol, respectively. Molecular orientation relative to the metal cluster only modestly affects the vibrational frequencies. As might be expected, the upright position wavenumbers differed from the isolated molecule on an average of 3 cm^{-1} for both benzenethiol and 4-mercaptophenol. The greatest deviation from the isolated molecule for this orientation of benzenethiol was 9.6 cm^{-1} for out-of-plane H bends and 8.6 cm^{-1} for the C−S stretch and ring-opening mode. The orientation with the ring in proximity to the metal cluster had on average 6.4 and 9.9 cm^{-1} difference between the isolated molecules for benzenethiol and 4-mercaptophenol, respectively. The greatest deviations of 17.3 and 17.3 cm^{-1} from the isolated molecule arose from the C−H ring "twist" and the C−C ring stretch for benzenethiol. For 4-mercaptophenol, deviations of 25 cm^{-1} from the isolated molecule occurred in the C−S stretch and ring-opening mode and the C−C ring stretch with a bend on the hydroxyl hydrogen. The greatest difference in frequency between the two molecular orientations is for the C−C stretch ring deformations with a difference of 20 cm^{-1}. For the experimental benzenethiol data, there are only modest differences between the SERS spectrum and the standard Raman spectrum of the neat material. For the major peaks in the neat spectrum at 413, 999, 1023, 1072, and 1583 cm^{-1}, the differences with the SERS spectrum are 2, 4, 4, 4, and 12 cm^{-1}, respectively. The minimal

dx.doi.org/10.1021/jp403458k | J. Phys. Chem. A XXXX, XXX, XXX−XXX

Table 1. Comparison of the Frequencies and Intensities of the "Up", "Down" Orientations and the Isolated Molecule of benzenethiol

benzenethiol						
up		down		single molecule		
cm^{-1}	$Å^4$/amu	cm^{-1}	$Å^4$/amu	cm^{-1}	$Å^4$/amu	
384.4	3992	386.3	2497	379.6	15	C−S stretch, ring stretch
401.7	29	402.7	1020	405.5	0.34	out-of-plane ring deformation
839.9	28	857.2	859	849.5	0.0124	symmetric out-of-plane H bends
972.5	810	960.0	173	973.5	39	trigonal ring breathing without C attached to S
997.5	2763	997.5	49	999.4	17	trigonal ring breathing with C attached to S
1052.3	9073	1047.5	61	1060.9	6.4	C−S stretch, ring-opening
1168.6	1085	1162.8	680	1168.6	3.9	C−H in-plane bends
1438.6	3035	1427.1	1120	1444.4	0.94	C−H ring "twist"
1562.6	11828	1547.2	402	1564.5	1.7	C−C ring stretch

Table 2. Comparison of the Frequencies and Intensities of the "Up", "Down" orientations and the isolated molecule of 4-mercaptophenol

4-mercaptophenol						
up		down		single molecule		
cm^{-1}	$Å^4$/amu	cm^{-1}	$Å^4$/amu	cm^{-1}	$Å^4$/amu	
407.5	3708	405.5	1630	414.2	0.43	out-of-plane ring deformation
804.4	527	817.8	502316	804.4	6.7	out-of plane H bend on hydroxyl side of ring
984.1	376479	986.0	0	985.0	1.922	trigonal ring breathing
1046.5	0	1034.0	228777	1059.0	1.2	C−S stretch, ring-opening
1122.4	171714	1120.5	13447	1122.4	6.1	O−H bend
1160.9	0	1157.0	332292	1161.8	5	in-plane C−H bends
1222.4	137012	1214.7	393413	1223.4	8	C−O stretch + ring breathing
1387.7	23	1372.3	111172	1389.6	0.27	in-plane C−H bends
1455.0	265747	1442.5	383479	1461.7	1.02	ring "twist"
1558.7	0	1538.6	110428	1563.5	16	C−C ring stretch, hydroxyl H bend
1584.7	162255	1573.2	850250	1585.7	24	C−C ring stretch

frequency differences between peaks in the SERS spectrum and the standard Raman spectrum of the neat compound are consistent with the frequency differences between the "up" oriented molecule in the model and the isolated benzenethiol molecule. Similar differences of 0, 1, 3, and 3 cm^{-1} are obtained between the SERS spectrum and the Raman spectrum of neat solid 4-mercaptophenol for several major peaks that could be reliably assigned at 634, 1008, 1170, and 1602 cm^{-1}, respectively. This indicates that both benzenethiol and 4-mercaptophenol are in an upright position. An upright position for benzenethiol is also consistent with the known structure of the benzenethiol SAM and the analysis of the relative peak intensities previously mentioned.[21]

More dramatic differences between molecular orientations can be observed in the predicted Raman activities, and the modeling results indicate that inferring molecular orientation from the differences in vibrational frequencies in the neat Raman and the SERS spectra could be difficult. For C−C ring stretching, C−S stretching/ring-opening, and out-of-plane ring deformation modes of benzenethiol at ∼1562.6, 1052.3, and 401.6 cm^{-1}, respectively, there is a nearly two orders of magnitude difference in intensities between the two orientations. The in-plane motions tend to be enhanced in the up orientation, and out-of-plane motions tend to enhanced for the down orientation. For some of the modes of 4-mercaptophenol involving motion of the ring carbons, most notably the in-plane H-bending mode, C−S stretch/ring-opening mode, and the C−C ring stretch with hydroxyl H bend at 1046.5, 1160, and 1558.7 cm^{-1}, respectively, the Raman activity is reduced to 0 for the up position. These same modes are dramatically enhanced for the down position. When the intensities of modes that are present in the normal Raman spectrum are reduced to nil in the SERS spectrum, it becomes difficult to determine which bands are present in both spectra and to determine frequency shifts.

Whereas the up spectra are closer in agreement to the experiment than the down spectra, there remains a significant difference between the experimental and predicted spectra. This shows that the orientation of the analyte molecule and the metal cluster does not fully account for features in the spectra.

Figure 8 compares the experimental benzenethiol on silver SERS spectrum to spectra calculated from a single benzenethiol and Ag atom to three benzenethiol molecules and three Ag atoms. The experimental spectrum has peaks at 416, 689, 986, 996, 1020, 1069, 1155, 1181, 1470, and 1571 cm^{-1} that we assign to a C−S bond and ring stretch, a C−S stretch and ring breathing mode, an out-of-plane H bend, a trigonal ring breathing mode, a trigonal breathing mode with out-of-plane C−H, a ring breathing mode, a ring twist mode, an antisymmetric twist mode, and a C−C ring stretch mode, respectively. These peaks appear in the theoretical spectra below the experimental one. The three theoretical spectra were calculated from the models shown, where the number of benzenethiol + Ag units is increased from one to three. The most striking observation that can be made is that as benzenethiol + Ag units are added to the model the relative

dx.doi.org/10.1021/jp403458k | J. Phys. Chem. A XXXX, XXX, XXX−XXX

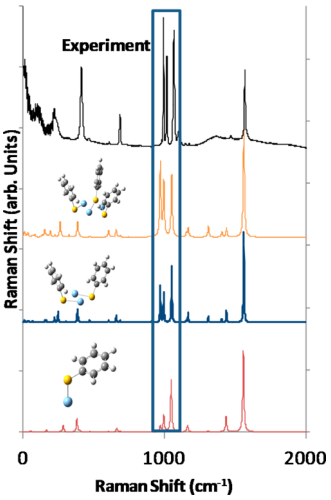

Figure 8. Effect of analyte−molecule interaction. Comparison of experimental and theoretical spectra of benzenethiol on silver. As intermolecular interaction between analyte molecules is increased, ring breathing and stretching modes become more pronounced.

intensities between the peaks at 970, 996, 1052, and 1560 cm^{-1}, begin to resemble the relative intensities of the experimental peaks at 996, 1020, 1069, and 1571 cm^{-1}, respectively.

The numbers in Table 3 show the degree of agreement between experiment and models for both the single analyte and

Table 3. SERS Frequencies and Relative Intensities

	experiment	one molecule	three molecules
	benzenethiol		
ω_1	997 cm^{-1}	969 cm^{-1}	972 cm^{-1}
$I(\omega_1)/I(\omega_1)$	1	1	1
ω_2	1019 cm^{-1}	995 cm^{-1}	996 cm^{-1}
$I(\omega_2)/I(\omega_1)$	0.696	3.195	0.75
ω_3	1069 cm^{-1}	1049 cm^{-1}	1053 cm^{-1}
$I(\omega_3)/I(\omega_1)$	0.897	10.512	0.82
ω_4	1571 cm^{-1}	1559 cm^{-1}	1560 cm^{-1}
$I(\omega_4)/I(\omega_1)$	0.537	16.341	1.228
	4-mercaptophenol		
ω_1	1006 cm^{-1}	985 cm^{-1}	984 cm^{-1}
$I(\omega_1)/I(\omega_1)$	1	1	1
ω_2	1078 cm^{-1}	1044 cm^{-1}	1049 cm^{-1}
$I(\omega_2)/I(\omega_1)$	7.892	7.828	11.711
ω_3	1069 cm^{-1}	1049 cm^{-1}	1053 cm^{-1}
$I(\omega_3)/I(\omega_1)$	0.411	1.005	1.23
ω_4	1599 cm^{-1}	1580 cm^{-1}	1586 cm^{-1}
$I(\omega_4)/I(\omega_1)$	2.097	10.729	12.19

metal atom system and for the three analyte molecule and three-metal-atom systems that appear in Figure 8. The frequencies listed in Table 3 correspond to similar vibrational modes in both benzenethiol and 4-mercaptophenol. Interestingly, ω_1 through ω_3 correspond to ring-breathing modes, and ω_4 corresponds to a ring-stretching mode with stretching along the two C−C bonds parallel to the C−S bond. The intensities have been normalized using the intensity of ω_1. For the ω_2, ω_3, and ω_4 frequencies of benzenethiol with a single analyte molecule, the predicted relative intensities are up to 30 times greater than what is seen experimentally. However, when three analyte molecules are considered together, the theoretical relative enhancements are much closer to the experimental values.

The result points toward a key assumption in the previous simulations that the benzenethiol and 4-mercaptophenol surface densities are low so that there is no interaction between these molecules. X-ray studies have shown that in fact SAMs from aromatic thiols form densely packed, highly ordered structures on noble-metal surfaces such as silver.[24] Furthermore, the 24.5° cant angle between the molecule and the vector normal to the substrate shows that the molecules are tightly packed, where isolated molecules tend to come into contact with the substrate. Because the packing of the benzenethiol molecules forces them to be in the upright position, they must be close enough to influence the electronic structure of each other and thus the degree of Raman enhancement as well. Figure 9 shows the highest occupied molecular orbital (HOMO) and the two MOs immediately below the HOMO in energy for both benzenethiol and 4-mercaptophenol. It can be seen that sharing of electron density occurs across all three model molecules for both analyte compounds. This result demonstrates that interaction between analyte molecules on the SERS substrate surface should be included and that charge-transfer states can be considered to involve groups of molecules and the metal substrate. In the sum of states framework, these charge-transfer states contribute to the sum over the ground and excited electronic and nuclear states.[14]

Although the model of three benzenethiol molecules plus three Ag atoms helps explain how interaction between benzenethiol molecules influences the contribution of the ring breathing modes to the peaks at 970, 996, and 1052 cm^{-1} in the experimental spectrum, this model is not sufficient to explain a number of features in the experimental spectrum. The C−S bond stretch/ring stretch modes at 416 and 657 cm^{-1} in the theoretical spectra are much less intense than the corresponding peaks in the experimental spectrum. A critical difference between the model and experiment is that the model does not have a surface and that there is no surface to constrain motion of the sulfur atom along the C−S bond stretch. In contrast with the ring breathing modes, where the sulfur "anchor" does not move, the modes at 416 and 657 cm^{-1} involve motion of sulfur atoms, and the presence of a metal surface becomes relevant. Interaction with the substrate surface likely accounts for the greater experimental intensities compared with the theoretical spectra.

There are a number of differences in vibrational frequency and intensity between the spectra calculated from the models and the experimental spectrum between 1150 and 1500 cm^{-1}. The theoretical spectra have five peaks at 1160, 1173, 1311, 1409, and 1422 cm^{-1} that have much greater intensity than the three small peaks at 1150, 1178, and 1470 cm^{-1} in the experimental spectrum. The normal-mode motion of all five theoretical peaks involves significant in-plane H bends. The three-benzenethiol-molecule model permits the electronic structure of several molecules to interact and contribute to the Raman spectrum, but it does not necessarily emulate the intermolecular interactions in the structure of the SAM formed by benzenethiol on silver. In contrast with the ring-breathing modes that are dominated by displacement of the carbon atoms, the peaks in between 1150 and 1500 cm^{-1} involve significant motion of the hydrogen atoms. It is reasonable to suggest that these modes experience greater perturbation from the structure of the SAM than the ring-breathing modes. It

dx.doi.org/10.1021/jp403458k | J. Phys. Chem. A XXXX, XXX, XXX−XXX

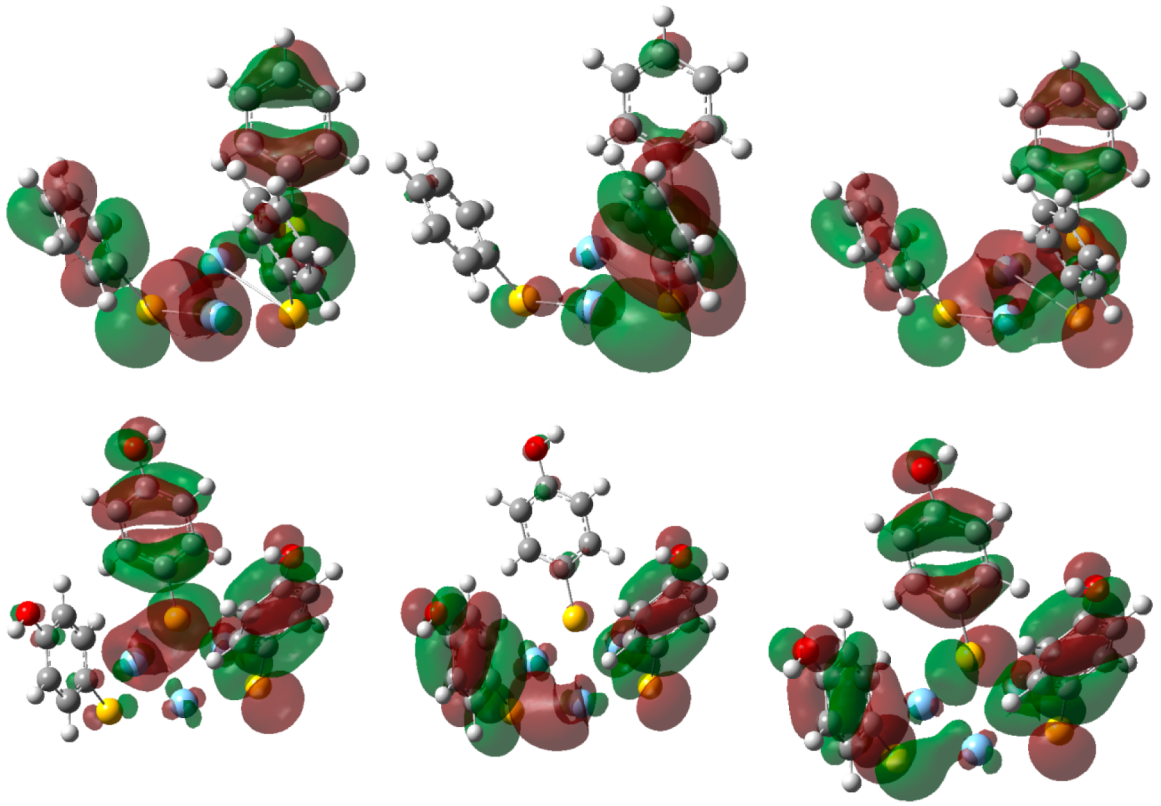

Figure 9. Three highest energy occupied molecular orbitals distributed over the three-membered cluster of benzenethiol/Ag (top three) and 4-mercaptophenol/Ag (bottom three) showing integration of the electronic structure of multiple analyte molecules.

seems a more accurate model of the SAM/surface structure is necessary to emulate the experimental SERS spectrum.

Although the inclusion of interaction between benzenethiol molecules is critical for making theoretical spectra conform to experiment, inclusion of multiple 4-mercaptophenol molecules in our model has little effect. The theoretical spectra in Figure 10 show little change as 4-mercaptophenol plus Ag units are added to the model. Eight well-defined peaks appear at 389, 633, 818, 1007, 1077, 1168, 1489, and 1598 cm^{-1} in the experimental spectrum. A ninth peak appearing as a shoulder on the peak at 1598 cm^{-1} appears at 1584 cm^{-1}. These can be matched to peaks in the theoretical spectra appearing at 358, 589, 786, 982, 1050, 1123, 1456, and 1587 cm^{-1}, respectively. A peak close to the one at 1587 cm^{-1} appears at 1560 cm^{-1} and could be identified with the shoulder on the 1598 cm^{-1} peak in the experimental spectrum.

As shown in Table 3, the relative intensities of the theoretical spectra for ω_2 of the one- and three-molecule models are close to the experimentally observed value. For the relative intensities of ω_3 and ω_4, increasing the number of analyte molecules in the model from one to three does not bring the theoretical spectra into agreement with experiment. As a result, merely allowing intermolecular interaction does not account for some of the features in the 4-mercaptophenol spectrum. There are two possibilities that need to be investigated for 4-mercaptophenol. First, and most likely, the true structure of the 4-mercaptophenol on the substrate surface may not have been captured in the theoretical model. The results of the benzenethiol simulation indicate that local molecular environment is important and that the structure of the SAM affects which vibrational modes experience enhancement. The theoretical model shown in Figure 10 probably does not

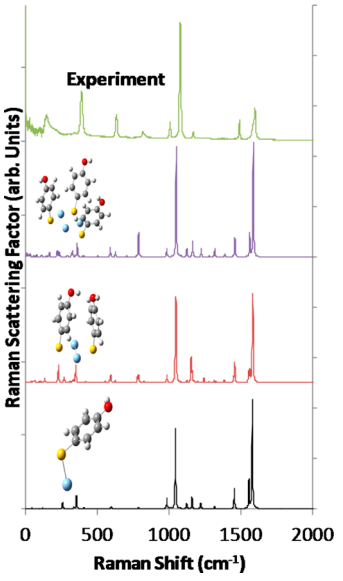

Figure 10. Effect of analyte molecule interaction on the 4-mercaptophenol on silver system. For this system, there is little change in the theoretical SERS spectrum as more 4-mercaptophenol molecules are added to the model.

reflect the real structure. The alcohol group can form hydrogen bonds and can force the monolayer to have a particular orientation and structure. Whereas there appears to be interaction between two of the 4-mercaptophenol molecules in the two-molecule model in Figure 10, this single linkage may be insufficient to accurately model the true structure. A second possibility is that the alcohol group changes the polarity of the

dx.doi.org/10.1021/jp403458k | J. Phys. Chem. A XXXX, XXX, XXX–XXX

molecule so much that the electronic structure of the analyte molecule is less affected by the local environment. Future work on this system will investigate these two possibilities.

CONCLUSIONS

We have performed a dual experimental and theoretical study of SERS spectra of benzenethiol and 4-mercaptophenol on silver substrates to gain insight into the factors that enhance a given vibrational mode when an analyte molecule chemically binds to the SERS substrate. The most important finding for the benzenethiol on silver system is that interaction between analyte molecules must be included to account for relative enhancements at 995, 1019, 1069, and 1571 cm^{-1}. For the 4-mercaptophenol on silver system, there was not a clear connection between the predicted SERS spectra and the experiment. We attribute the difference between model and experiment to differences between the model geometry and the real 4-mercaptophenol structure on the SERS substrate surface or to alcohol-group-induced changes in the electronic structure of the molecule arising from modifications to the molecular polarity. Second, the effect of molecular orientation relative to the SERS surface has been investigated for both benzenethiol and 4-mercaptophenol. A comparison between experiment and theoretical SERS spectra shows that theoretical models where the analyte molecules are upright are in best agreement experiment. An analysis of vibrational frequency shifts between the model including an "up" and "down" orientation of the molecules relative to the seven-Ag-atom cluster, and a model of the free molecule shows little perturbation and is also consistent with an upright position. An upright orientation of benzenethiol is consistent with studies on SAMS formed from these thio compounds.

Using closed-shell calculations, the influence of metal cluster size was investigated using benzenethiol and 4-mercaptophenol associated with one-, three-, five-, and seven-atom silver clusters. We found little consistent dependence of the relative enhancements on the cluster size, where best agreement with experiment was found with a single silver atom. We attribute that result to weak and isolated charge-transfer states that appear at low energy and enter preresonance with the 785 nm excitation modeled in the calculation. These charge-transfer states are highly sensitive to the geometry between the analyte molecule and the SERS substrate, and resonance and preresonance with these states can greatly affect the appearance of the predicted SERS spectrum. The effect of these charge-transfer states can be overemphasized in models with a small ensemble of analyte molecules.

While we find that interaction between analyte molecules on a substrate can impact the relative chemical enhancements within the SERS spectrum and should be accounted for, we also confirm other studies that find that the overall SERS spectrum is highly sensitive to the local environment around the molecule.

AUTHOR INFORMATION

Notes

The authors declare no competing financial interest.

ACKNOWLEDGMENTS

We acknowledge internal funding provided by ECBC's In-house Laboratory Independent Research (ILIR) program administered by Dr. A. W. Fountain III as well as High Performance Computing resources provided by the Department of Defense Supercomputing Resource Center (DSRC) that is funded through the PETTT program.

REFERENCES

(1) Zhao, L. L.; Jensen, L.; Schatz, G. C. Pyridine-Ag-20 Cluster: A Model System for Studying Surface-Enhanced Raman Scattering. *J. Am. Chem. Soc.* **2006**, *128*, 2911−2919.

(2) Maitani, M. M.; Ohlberg, D. A. A.; Li, Z.; Allara, D. L.; Stewart, D. R.; Williams, R. S. Study of SERS Chemical Enhancement Factors Using Buffer Layer Assisted Growth of Metal Nanoparticles on Self-Assembled Monolayers. *J. Am. Chem. Soc.* **2009**, *131*, 6310−6311.

(3) Lombardi, J. R.; Birke, R. L.; Lu, T.; Xu, J. Charge-Transfer theory of Surface Enhanced Raman Spectroscopy: Herzberg-Teller Contributions. *J. Chem. Phys.* **1986**, *84*, 4174−4180.

(4) Birke, R. L.; Znamenskiy, V.; Lombardi, J. R. A Charge-Transfer Surface Enhanced Raman Scattering Model from Time-Dependent Density Functional Theory Calculations on a Ag_{10}-Pyridine Complex. *J. Chem. Phys.* **2010**, *132*, 214707−1.

(5) Aroca, R. F.; Clavijo, R. E. Surface-Enhanced Raman Spectra of Phthalimide. Interpretation of the SERS Spectra of the Surface Complex Formed on Silver Islands and Colloids. *J. Phys. Chem. A* **2000**, *104*, 9500−9505.

(6) Saikin, S. K.; Oliveres-Amaya, R.; Rappoport, D.; Stopa, M.; Aspuru-Guzik, A. On the Chemical Bonding Effects in the Raman Response: Benzenethiol Adsorbed on Silver Clusters. *Phys. Chem. Chem. Phys.* **2009**, *11*, 9401−9412.

(7) Saikin, S. K.; Chu, Y.; Rappoport, D.; Crozier, K. B.; Aspuru-Guzik, A. Separation of Electromagnetic and Chemical Contributions to Surface-Enhanced Raman Spectra on Nanoengineered Plasmonic Substrates. *J. Phys. Chem. Lett.* **2010**, *1*, 2740−2746.

(8) Morton, S. M.; Jensen, L. Understanding the Molecule-Surface Chemical Coupling inSERS. *J. Am. Chem. Soc.* **2009**, *131*, 4090−4098.

(9) Silverstein, D. W.; Jensen, L. Understanding the Resonance Raman Scattering of Donor-Acceptor Complexes Using Long-Range Corrected DFT. *J. Chem. Theor. Comput.* **2010**, *6*, 2845−2855.

(10) Cardini, G.; Muniz-Miranda, M.; Pagliai, M.; Schettino, V. A Density Functional Study of the SERS Spectra of Pyridine Adsorbed on Silver Clusters. *Theor. Chem. Acc.* **2007**, *117*, 451−458.

(11) Johansson, P. Illustrative Direct Ab Anitio Calculations of Surface Raman Spectra. *Phys. Chem. Chem. Phys.* **2005**, *7*, 475−482.

(12) Vivoni, A.; Birke, R. L.; Foucault, R.; Lombardi, J. R. Ab Initio Frequency Calculations of Pyridine Adsorbed on an Adatom Model of a SERS Active Site of a Silver Surface. *J. Phys. Chem. B* **2003**, *107*, 5547−5557.

(13) Lombardi, J. R.; Birke, R. L. A Unified View of Surface-Enhanced Raman Scattering. *Acc. Chem. Res.* **2009**, *42*, 734−742.

(14) Albrecht, A. C. On the Theory of Raman Intensities. *J. Chem. Phys.* **1961**, *34*, 1475−1484.

(15) Carrasco-Flores, E. A.; Campos Vallette, M. M.; Clavijo, R. E. C.; Leyton, P.; Diaz, G.; Koch, R. SERS Spectrum and DFT Calculations of 6-Nitrochrysene on Silver Islands. *Vib. Spectrosc.* **2005**, *37*, 153−160.

(16) Chien, F. C.; Huang, W. Y.; Shiu, J. Y.; Kuo, C. W.; Chen, P. Revealing the Spatial Distribution of the Site Enhancement for the Surface Enhanced Raman Scattering on the Regular Nanoparticle Arrays. *Opt. Express* **2009**, *17*, 13974−13981.

(17) Cardini, G.; Muniz-Miranda, M. Density Functional Study on the Adsorption of Pyrazole onto Silver Colloidal Particles. *J. Phys. Chem. B* **2002**, *106*, 6875−6880.

(18) Kambhampati, P.; Child, C. M.; Foster, M. C.; Campion, A. On the Chemical Mechanism of Surface Enhanced Raman Scattering: Experiment and Theory. *J. Chem. Phys.* **1998**, *108*, 5013−5026.

(19) Payton, J. L.; Morton, S. M.; Moore, J. E.; Jensen, L. A Discrete Interaction Model/Quantum Mechanical Method for Simulating Surface-enhanced Raman Spectroscopy. *J. Chem. Phys.* **2012**, *136*, 214103−1.

(20) Ling, X.; Wu, J.; Xu, W.; Zhang, J. Probing the Effect of Molecular Orientation on the Intensity of Chemical Enhancement Using Graphene-Enhanced Raman Spectroscopy. *Small* **2012**, *8*, 1365−1372.
(21) Love, J. C.; Estroff, L. A.; Kriebel, J. K.; Nuzzo, R. G.; Whitesides, G. M. Self-Assembled Monolayers of Thiolates on Metals as a Form of Nanotechnology. *Chem. Rev.* **2005**, *105*, 1103−1169.
(22) Barriet, D.; Yam, C. M.; Shmakova, O. E.; Jamison, A. C.; Lee, T. R. 4-Mercaptophenylboronic Acid SAMs on Gold: Comparison with SAMs Derived from Thiophenol, 4-Mercaptophenol, and 4-Mercaptobenzoic Acid. *Langmuir* **2007**, *23*, 8866−8875.
(23) Harb, M.; Rabilloud, R.; Simon, D. Optical Response of Silver Nanoclusters Complexed with Aromatic Thiol Molecules: A Time-Dependent Density Functional Study. *J. Phys. B* **2011**, *44*, 035101.
(24) Frey, S.; Stadler, V.; Heister, K.; Eck, W.; Zharnikov, M.; Grunze, M. Structure of Thioaromatic Self-Assembled Monolayers on Gold and Silver. *Langmuir* **2001**, *17*, 2408−2415.
(25) Lee, P. C.; Meisel, D. Adsorption and Surface-Enhanced Raman of Dyes and Gold Sols. *J. Phys. Chem.* **1982**, *86*, 3391−3395.
(26) Guicheteau, J.; Argue, L.; Emge, D.; Hyre, A.; Jacobson, M.; Christesen, S. Bacillus Spore Classification Via Surface-enhanced Raman Spectroscopy and Principal Component Analysis. *Appl. Spectrosc.* **2008**, *62*, 267−272.
(27) Frisch, M. J., Trucks, G. W., Schlegel, H. B., Scuseria, G. E., Robb, M. A., Cheeseman, J. R., Scalmani, G., Barone, V., Mennucci, B., Petersson, G. A., et al. *Gaussian 2009*, revision C.01; Gaussian, Inc.: Wallingford, CT, 2009.
(28) NIST Computational Chemistry Comparison and Benchmark Database, NIST Standard Reference Database Number 101, Release 15b; Johnson, R. D.,III, Ed.; NIST: Gaithersburg, MD, 2011. http://cccbdb.nist.gov/.